Antimicrobial Hybrid Coatings Combining Enhanced Biocidal Activity Under Visible Light Irradiation with Self-Renewable Properties

Journal:	*ACS Applied Materials & Interfaces*
Manuscript ID	am-2020-08365j
Manuscript Type:	Article
Date Submitted by the Author:	07-May-2020
Complete List of Authors:	Manouras, Theodore; University of Crete School of Sciences and Engineering, Department of Materials Science and Technology Koufakis, Eleftherios; University of Crete School of Sciences and Engineering, Department of Materials Science and Technology Vasilaki, Evangelia; University of Crete School of Sciences and Engineering, Materials Science and Technology Peraki, Ioanna; Foundation of Research and Technology Hellas, Institute of Molecular Biology and Biotechnology Vamvakaki, Maria; University of Crete School of Sciences and Engineering, Materials Science and Technology

Antimicrobial Hybrid Coatings Combining Enhanced Biocidal Activity Under Visible Light Irradiation with Self-Renewable Properties

Theodore Manouras,[1,2] Eleftherios Koufakis,[1,2] Evangelia Vasilaki,[1,2] Ioanna Peraki[3] and Maria Vamvakaki[1,2,]*

[1]Institute of Electronic Structure and Laser, Foundation for Research and Technology–Hellas, 700 13 Heraklion, Crete, Greece

and

[2]Department of Materials Science and Technology, University of Crete, 700 13 Heraklion, Crete, Greece

and

[3]Institute of Molecular Biology and Biotechnology, Foundation for Research and Technology – Hellas, 700 13 Heraklion, Crete, Greece

submitted for publication in *ACS Applied Materials and Interfaces*

*email: vamvakak@iesl.forth.gr

Abstract

Hybrid, organic-inorganic, biocidal films, exhibiting self-polishing properties, were developed as effective long-lasting antimicrobial surface coatings. The films were prepared using cationically modified chitosan, synthesized by the reaction with3-bromo-*N,N,N*-trimethylpropan-1-aminium bromide, to introduce permanent biocidal quaternary ammonium salt (QAS) groups along the polymer backbone, and were cross-linked by a novel, pH-degradable acetal-based cross-linker, which enabled the pH-responsive self-polishing of the hybrid coatings. TiO_2 nanoparticles, modified with reduced graphene oxide (rGO) sheets, to narrow their band gap energy value and shift their photocatalytic activity in the visible light regime, were introduced within the polymer film to enhance its antibacterial activity. The hybrid coatings exhibited an effective biocidal activity in the dark (98% killing of Gram-negative and 99.9% killing of Gram-positive bacteria), when only the cationic polymer sites interacted with the bacteria membrane, and an excellent biocidal action upon visible light irradiation (99,999% killing of Gram-negative and 99.9999% killing of Gram-positive bacteria) due to the synergistic antimicrobial effect of the QAS moieties and the rGO-modified TiO_2 nanoparticles. Finally, a gradual decrease in the film thickness was found, when the coatings were immersed in mildly basic (pH 8), neutral (pH 7) and acidic (pH 6) media, reaching 10, 20 and 70 % reduction, respectively after 60 days immersion time, verifying the self-polishing behavior of the coatings and the renewal of their antimicrobial surface.

Keywords: quaternized chitosan, TiO_2, reduced graphene oxide, acetal-based cross-linker, biocidal surfaces, self-renewable antimicrobial coatings

Introduction

Microbial infectious diseases often occur as a result of the contamination of surfaces by a plethora of pathogens, and constitute a growing threat to human health, with major risks in food packaging and storage, water filtration-purification, household sanitation and the biomedical field. Bacterial biofilm formation has been identified as the profound event of microbial contaminated surfaces. This emerging threat has triggered research towards the development of effective, long-lasting and environmentally friendly bacteria elimination surfaces.[1-4]

Initial studies have focused on antifouling coatings that repel the microorganisms, preventing their attachment on the surface and thus the formation of the biofilm. Superhydrophilic and superhydrophobic surfaces have been reported to present such a barrier for bacteria adhesion, however, these surfaces do not eliminate the problem of bacterial contamination, but rather relocate it to an unmodified surface site.[5-6]

A more effective approach for the development of antimicrobial surfaces employs materials that can kill the microorganisms.[7] Such surfaces are known as biocidal surfaces or antimicrobial surfaces with biocidal activity. The contact killing action of biocidal surfaces is induced by the interaction of biocidal moieties present on the surface with the outer cell membrane of the microorganisms, leading to its destabilization and disruption, and therefore to the necrosis of the bacteria.[8] A plethora of inorganic and organic materials have been developed for use as effective biocidal systems. The former include metal and metal oxide nanoparticles, such as silver, gold, copper, ZnO and TiO_2.[9-13] Photocatalytic TiO_2 nanoparticles have been systematically investigated in the recent years, exhibiting certain advantages, such as a broad spectrum of antimicrobial action against Gram-positive and Gram-negative bacteria and fungi, commercial availability and low cost.[14-15] However, an important disadvantage of TiO_2 is its large band gap energy (~ 3.2 eV) which requires the use of UV light to activate its

antimicrobial action.[16-17] On the other hand, organic biocidal materials comprise antimicrobial peptides, natural products, polymers, and others.[18-20] Synthetic antimicrobial polymers with biocidal properties are usually cationic polyelectrolytes, based on quaternary phosphonium and ammonium salt moieties, which kill the microbes by disrupting their negatively charged membrane.[21] They provide significant benefits for the development of antimicrobial surfaces, such as chemical stability, facile processing, a broad spectrum of antimicrobial effectiveness and long-lasting activity.[22] However, they also possess important disadvantages, i.e. low biocompatibility for mammalian cells, non-degradability, complex synthesis and high cost. Natural polymers have emerged as an important class of materials to address the above challenges, because they combine biocompatibility, biodegradability, commercial availability and low cost, rendering them ideal candidates for use in antimicrobial surfaces.[23-24] Among them, chitosan is a naturally abundant biopolymer with promising antimicrobial properties.[25] Chitosan is insoluble in basic and neutral water, but dissolves in acidic media, upon the protonation of the primary amine groups along the polymer chain.[26] These positively charged polymer moieties can effectively interact with the anionic cell membrane of the pathogenic microorganisms, causing its destabilization, which leads to pathogen necrosis.[27-29] The use of chitosan in the development of antimicrobial surfaces has been extensively reported,[30-32] however, its antimicrobial activity is only effective in acidic environments, at which the polymer acquires a positive charge, and deteriorates in neutral and basic media, when the amine groups are neutral.[33] To address the above limitation, and improve the antimicrobial properties of chitosan, its modification to bear permanent cationic sites along the polymer chain has been proposed via quaternization, carboxymethylation, and cationization reactions.[34]

A major drawback of contact-killing antimicrobial surfaces is the deterioration of their effectiveness with time, due to the accumulation of the debris of the killed bacteria, which hinders the effective interaction of the surface with alive bacteria. To overcome the problem of

dead bacteria deposition, a promising "kill-and-release" strategy has been proposed, for the development of surfaces with long-term antibacterial activity.[35-36,37-42] In this approach, an appropriate stimulus is employed to release dead bacteria and the debris from the surface, providing a promising solution for the prevention of initial bacterial attachment and subsequent biofilm formation. Wang et al.[43] developed a smart antibacterial surface exhibiting NIR-induced photothermal killing, based on a tannic acid/Fe complex, and a thermally triggered release of the dead bacteria, due to the lower critical solution temperature transition of poly(N-isopropylacrylamide) grafted chains on the surface. In another study, Yan et al.[44] prepared a bacteria-responsive antimicrobial surface based on an antimicrobial peptide (AMP) inner layer and a poly(methacrylic acid) (PMAA) outer layer. The hydrated PMAA layer resisted initial bacterial attachment, whereas, upon microbial colonization on the surface, the bacteria-triggered acidification or the PMAA layer caused its collapse and the exposure of the underlying bactericidal AMP layer, which killed the attached bacteria.

In the present work, we report the development of a hybrid coating presenting excellent biocidal efficacy, and the ability to self-polish, and therefore regenerate its outer surface, overcoming the severe problem of dead bacterial deposition. The coating comprises chitosan, modified with *N,N,N*-trimethylpropan-1-aminium bromide to introduce permanent cationic biocidal groups along the polymer chain, and TiO_2 nanoparticles, modified with reduced graphene oxide (rGO),to narrow their band gap energy and shift their photocatalytic activity in the visible light regime. The hybrid coating was cross-linked using a novel acid-degradable, acetal-based cross-linker, which reacted with the free amine functionalities of chitosan. The hybrid films were assessed in terms of their antibacterial action in the dark and under visible light irradiation. The self-polishing behavior of the films, to remove the contamination induced by the dead bacteria deposition, and renew their top surface, was studied as a function of the pH of the medium.

Experimental Section

Materials

All reagents were of analytical grade and were used as received. Chitosan (degree of deacetylation (DD) 85%) was purchased from Glentham Life Sciences and 3-bromo-*N,N,N*-trimethylpropan-1-aminium bromide was obtained from Fluorochem. Sodium hydroxide, tri(ethylene glycol) divinyl ether, 2-bromoethanol, pyridinium *p*-toluenesulfonate, hydrogen peroxide, sulfuric acid, (3-glycidyloxypropyl)trimethoxysilane (GOPTES), titanium(IV)isopropoxide (TIP), sodium nitrate, graphite, potassium permanganate, tryptone, sodium chloride, yeast extract, PBS, sodium cacodylate and all solvents used were purchased from Sigma Aldrich. The Live/Dead BacLight bacterial viability kit L7012 was obtained from Molecular Probes. Dialysis membranes with molecular weight cut-off (MWCO) 3500 g/mol were supplied from Medicell Membranes Ltd. Milli-Q water, obtained from a Millipore apparatus, with a resistivity of 18.2 MΩ.cm at 298 K was used for all experiments.

Modification of chitosan

Chitosan (2 g) was dispersed in 30 ml water at 85°C. 3-bromo-*N,N,N*-trimethylpropan-1-aminium bromide (2 g)was dissolved in water (10 ml) and was added in the chitosan dispersion. After stirring for 8h, the reaction became clear and attained a light-yellow color. Next, the pH was adjusted to 9 by the addition of NaOH (5M), which led to an increase of the turbidity of the solution, before adding another 10 ml of the aqueous 3-bromo-*N,N,N*-trimethylpropan-1-aminium bromide solution. After 10 h, the reaction mixture became clear again, and was dialyzed (MWCO 3500 g/mol), first against water for 2 days, then against aqueous NaOH (0.05 M) for 1 day, and finally against water for another 2 days, to remove the unreacted 3-bromo-*N,N,N*-trimethylpropan-1-aminium bromide. The product was isolated by precipitation in acetone, was filtered and was dried under vacuum for 24 h before use.

Synthesis of the acetal-based cross-linker

The synthesis of the acetal-based cross-linker was carried out by the catalyzed reaction of 2-bromoethanol with tri(ethylene glycol) divinyl ether to form the acetal linkages. For this, 2-bromoethanol (1.4 ml, 20 mmol) and tri(ethylene glycol) divinyl ether (2.0 ml, 10 mmol) were dissolved in 30 mL anhydrous tetrahydrofuran to obtain a 1.0 M solution. Next, a catalytic amount of pyridinium *p*-toluenesulfonate (1mol% with respect to tri(ethylene glycol) divinyl ether) was added in the reaction, and the solution was allowed to stir at room temperature for 24 h. Finally, the solution was neutralized with triethylamine, was passed through a basic alumina column to remove the catalyst, and the solvent was evaporated under vacuum to obtain the pure product.

Synthesis of rGO-modified TiO_2 nanoparticles

The procedure for the synthesis of the TiO_2 nanoparticles was adapted from the work of Wang et al.[45] Briefly, TIP (4 mL) was dissolved in 4 mL ethanol and the solution was added dropwise in 30 mL 1:2 EtOH:H_2O mixture (water:alkoxide molar ratio ~80) under vigorous stirring. The turbidity of the solution increased instantly and the dispersion was left under stirring for 2 h. Next, the TiO_2 nanoparticles were filtered, and were washed five times with ethanol and twice with H_2O, before being dried in a vacuum oven. Finally, crystallization of the amorphous TiO_2 nanoparticles to the anatase phase was induced by thermal annealing at 600 °C for 2 h under air, at a heating and cooling rate of ~5 °C/min.

Graphene oxide was synthesized from graphite by a modified Hummers' method.[46] Hydrothermal treatment was employed for the modification of the TiO_2 nanoparticles with rGO.[47] First, the TiO_2 nanoparticles were dispersed in a1:2 EtOH:H_2O mixture by ultrasonic treatment, while an aqueous GO suspension was prepared by ultrasonic treatment of GO in water (0.5 mg GO/ml H_2O) for 1 h. Next, an appropriate volume of the GO suspension was

added to the TiO_2 dispersion, to obtain a 4 wt% loading of GO onto the TiO_2 nanoparticles, and the mixture was stirred for 2 h. Finally, the GO-modified TiO_2 nanoparticles were hydrothermally treated at 120 °C for 24 h in a teflon-lined stainless-steel autoclave, to reduce GO to rGO.

Preparation of the hybrid films

The silicon and glass substrates used for the deposition of the hybrid films, were modified to bear surface epoxy anchoring units. For this, the substrates were first sonicated in 2-propanol for 10 min, dried with nitrogen and then cleaned with a freshly prepared 1:1 v/v H_2SO_4/H_2O_2 piranha solution (Caution! Piranha solution reacts violently with organic matter) for 30 min to remove any organic residues and increase the density of the reactive silanol groups on the surface. Next, the clean surfaces were rinsed extensively with water to completely remove the piranha solution. The substrates were dried under a nitrogen stream and were placed in a 1 v/v% solution of GOPTES in anhydrous toluene at 25 ºC. After 24h, the substrates were removed from the solution, washed with toluene and 2-propanol, to remove the unattached GOPTES molecules, followed by drying at 120 ºC under a nitrogen stream for 30 min.

The hybrid films were prepared on freshly cleaned and epoxy functionalized substrates as following: modified chitosan was dissolved in a 1:1 EtOH:H_2O mixture to yield a 5 wt% solution. Next, a 10 w/v% solution of the acetal-based cross-linker in ethanol was added at a 5 mol% cross-linker with respect to the moles of the chitosan repeat units, followed by the addition of 2 wt% rGO-modified TiO_2 nanoparticles (as a 0.2wt% dispersion in 1:1 EtOH:H_2O) with respect to chitosan. The final concentration of the solution was adjusted to 0.1 w/v% solids by the addition of a 1:1 EtOH:H_2O mixture. The hybrid films were prepared by drop casting the above solution on the substrates followed by baking at 50 °C on a hotplate to remove the solvents. Finally, the films were cured at 110 ^oC overnight in a vacuum oven and were next,

sonicated in ethanol for 5 min to remove any uncross-linked polymer before being dried under a nitrogen steam.

Characterization

Nuclear Magnetic Resonance (NMR) Spectroscopy

Proton Nuclear Magnetic Resonance (^{1}H NMR) spectra were measured using a Bruker Advance DPX 300 NMR Spectrometer (300 MHz) at 25 ^{o}C. 99.9% deuterium oxide (D_2O) or 99.9% deuterated chloroform ($CDCl_3$) were used as the solvents.

Attenuated Total Reflection Fourier Transform Infrared (ATR-FTIR) Spectroscopy

ATR-FTIR spectra of the rGO-modified nanoparticles and the hybrid films on silicon substrates were recorded in the 4000-400 cm^{-1} range with a resolution of 4 cm^{-1} using a Perkin Elmer, Model Frontier, FTIR spectrometer. In the self-polishing experiments of the hybrid coatings, the film thicknesses, following immersion in water of different pH values, were calculated by the decrease of the intensity of the peak at 1107 cm^{-1} which corresponds to the C-O-C stretching vibration attributed to chitosan and the acetal cross-linker.

Film thickness measurements

Ellipsometric measurements were performed on a variable angle spectroscopic ellipsometer (SE) (model VASE, J. A. Woolam Co., Inc.) to determine the thickness of the hybrid coatings. The angle of incidence was set to 70^{o}in the 450-1200 nm wavelength range. An average of five readings, collected from different locations of the sample, is reported.

Water contact angle measurements

Wettability was assessed by static water contact angle (WCA) measurements using a contact angle goniometer (OCA-40, Dataphysics) and the sessile drop method. A 5 μl droplet of nanopure water was used and the contact angles were calculated from the digital images of the water droplets deposited on the surfaces, recorded by a camera, using the appropriate software. All data are expressed as the mean values from triplicate experiments taken after drop equilibration.

X-ray Diffraction

X-ray diffraction (XRD) patterns of the TiO_2 and rGO-modified TiO_2 nanoparticles were measured on a PANalytical Xpert Pro X-ray diffractometer, using Cu Kα radiation (45kV and 40 mA).

Field Emission Scanning Electron Microscopy (FESEM)

Field emission scanning electron microscopy (FESEM) images were captured using a JEOL JSM-7000F field emission microscope at an accelerating voltage of 15 kV to visualize the morphology of the samples. A drop of the TiO_2 and rGO-modified TiO_2 nanoparticles was deposited on a glass slide and was dried overnight at room temperature. The dried samples were sputter-coated (SCD 050 Bal-Tec) with a 10 nm thick layer of Au to minimize charging during the measurements. The preparation of the bacteria samples for FESEM analysis is described below.

UV/Vis diffuse reflectance and UV/vis spectroscopies

UV/Vis diffuse reflectance spectra of the bare and the rGO-modified TiO_2 nanoparticles were measured using a Shimadzu UV-2401 PC spectrophotometer equipped with an ISR-240A

integrating sphere. A thin layer of the powder sample was deposited on the $BaSO_4$ reference material and the measurements were conducted in the 300-800 nm wavelength range.

UV/Vis absorption spectra of the hybrid films were obtained on a Perkin Elmer Lambda 25 spectrophotometer using quartz as the substrate. For all samples, the spectra were recorded between 200 and 500 nm at a1 nm interval.

Preparation of the Luria-Bertani medium and the Luria-Bertani agar plates

For the preparation of the Luria-Bertani (LB) medium, 1.0 g tryptone, 1.0 g sodium chloride and 0. 5 g yeast extract were dissolved in 100 ml water and the solution was autoclaved. After cooling down, the LB medium was stored at RT. For the preparation of the LB agar plates, 5 g tryptone, 5 g sodium chloride, 2.5 g yeast extract and 7.5 g agar were dissolved in 500 ml water and the solution was autoclaved. After cooling down to 40-45 ºC, 20 ml solution were poured into sterile plates of 10 cm diameter. The LB agar plates were conditioned at 4 ºC, for a maximum period of 1 month.

Antibacterial Tests

Two bacterial strains, *Bacillus cereus* (*B. cereus*) ATCC 14579 and *Escherichia coli* (*E. coli*), were chosen in the present study, as representative Gram-positive and Gram-negative bacteria, respectively. Both strains, were grown aerobically overnight in LB medium from frozen stocks. *B. cereus* and *E. coli* were cultivated, by streaking on LB agar plates followed by incubation at 37 ºC for 24 h. Next, individual colonies were obtained and were incubated in 3 ml LB culture medium. Both strains were shaken at 37 ºC for 24 h, and were next diluted with LB to obtain a predetermined concentration of 1×10^8 colony-forming units (CFU)/ml. The concentration of the bacteria was verified by serial dilutions and spreading onto agar plates, followed by the enumeration of the bacterial colonies. The antimicrobial activity of the hybrid films was

determined by measuring the CFU by the plate counting method (PCM), after 5 h contact of the bacteria with the films in the dark or under visible light irradiation (led light at 4000 K adjusted to 400 LUX) at 37 ^{o}C and is reported as the log reduction of the alive bacteria cells. Glass substrates were used as control surfaces under the same conditions. The samples were sterilized by immersion in ethanol and were dried by heating at 100 ^{o}C for 30 min. The samples were transferred to a sterile 12-well plate using sterilized forceps. 100 µl of the initial bacteria culture in PBS were deposited onto each sample. The samples were incubated in a thermostated cell culture chamber at 37 ^{o}C under a humidified atmosphere for 5 h in the dark or under visible light irradiation. Subsequently, both the suspension and the hybrid surface were placed in a falcon with glass sieves and were vortex stirred until the complete wreckage of the substrate. The suspension was diluted with PBS and 100 µl of each decimal dilution was spread onto sterile LB agar plates. The LB plates with the bacterial suspensions were incubated at 37 ^{o}C for 20 h to give visible colonies, which were enumerated to obtain the number of alive bacteria.

Fixation of bacteria for SEM analysis

The samples for FESEM were fixed with 2.5 % glutaraldehyde (GDA) in phosphate-buffered saline (PBS) at 4 ºC for 2 h and were dehydrated by gradually increasing the ethanol concentration from 30 to 100%. Next, the samples were dried, using a critical point dryer (CPD 030 Bal-Tec), and were finally sputter-coated (SCD 050 Bal-Tec) with a 10 nm thick layer of Pd-Au to minimize charging during the measurements.

Confocal Laser Scanning Microscopy (CLSM)

A spectral confocal laser scanning microscope (Leica DMi8 confocal microscope equipped with a green laser, red laser and analysis software LASXSmall3.7.1) and a Live/Dead BacLight bacterial viability kit L7012 (Molecular Probes) were used for the determination of the

live/dead attached bacteria onto the substrates. The attached bacteria were stained with a 1:1 v/v SYTO 9 dye (3.34 mM):propidium iodide (20 mM) in 0.85wt% NaCl. The SYTO 9 stain labels all bacteria, whereas propidium iodide penetrates the bacteria with a damaged membrane, thereby staining only the dead bacteria. Therefore, the SYTO 9 fluorescence is reduced when both dyes are present. After staining, the samples were incubated at room temperature in the dark for 15 min and were subsequently examined by CLSM.

Results and Discussion

Material Synthesis and Coating Preparation

Deacetylated chitosan (85% degree of deacetylation) was modified to bear quaternary ammonium salt (QAS) moieties, via a nucleophilic substitution reaction between 3-bromo-*N,N,N*-trimethylpropan-1-aminium bromide and the primary amine groups of the polymer, which leaves the hydroxyl groups of chitosan intact. The latter are known to play an important role in the biological activity of chitosan and its derivatives.[48] The fraction of alkylated amine groups was calculated from the ^{1}H NMR spectra of the modified polymer (Figure S1). The presence of an intense singlet at 2.9 ppm in the spectrum of the modified chitosan, attributed to the trimethylammonium protons, verified the successful substitution reaction. The degree of modification was calculated by ratioing the integrals of the D protons at 4.5 ppm, which correspond to the acetylated, deacetylated and alkylated monomer repeat units of chitosan, over the protons of the trimethylammonium group at 2.9 ppm, and the methyl protons of the acetylated units at 1.75 ppm. The final product comprised 15 mole% acetylated, 13 mole% deacetylated and 72 mole% alkylated monomer repeat units, signifying a high degree of modification and the presence of a large number of positively charged moieties along the polymer chain.

Next, an acetal-based bifunctional alkyl halide was designed and synthesized to be used as the cross-linker to chemically link the modified chitosan chains in the hybrid films and form a water insoluble polymer network. The acetal-based cross-linker was synthesized by the nucleophilic addition of 2-bromoethanol to tri(ethylene glycol) divinyl ether (Figures 1a and S2).

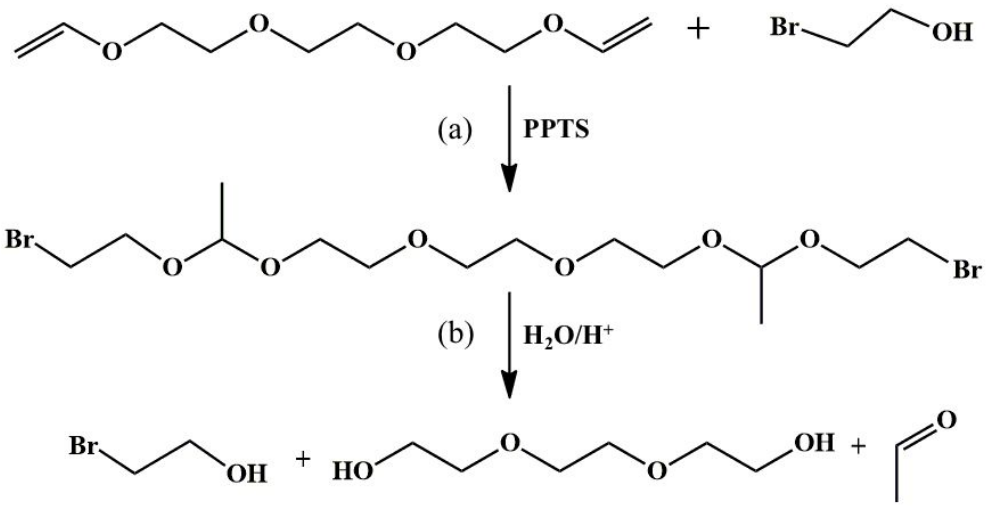

Figure 1: Schematic representation of the synthetic procedure followed for the preparation of the acetal-based cross-linker (a) and the degradation reaction of the cross-linker (b).

The polar tri(ethylene glycol) moiety of the cross-linker renders it soluble in the EtOH:H_2O mixture used to dissolve the modified chitosan. Furthermore, the cross-linker comprises two alkyl bromide functional groups which can react with the amine groups of chitosan, via an amine alkylation reaction, leading to the cross-linking of the polymer chains. Finally, the two acetal bonds of the cross-linker are well-known in the literature to hydrolyse under mildly acidic conditions to produce acetaldehyde and hydroxy compounds (Figure 1b).

rGO-modified TiO_2 nanoparticles were prepared by hydrothermal treatment and were characterized by SEM, ATR-FTIR and diffuse reflectance UV/vis spectroscopies as well as XRD measurements. The bare TiO_2 nanoparticles presented a spherical morphology with an

average diameter of ~60 nm by SEM (Figure S3a). After the modification of TiO_2 with rGO the successful attachment of the titania nanoparticles onto the graphitic sheets was verified by SEM (Figure S3b).

The ATR-FTIR spectra of the bare TiO_2 and the rGO-modified TiO_2 nanoparticles are shown in Figure S4. A characteristic band at ~450 cm^{-1} was observed in both spectra, assigned to the bending and stretching vibrations of the Ti–O and Ti–O–Ti framework bonds. For the rGO-modified TiO_2 nanoparticles, a new peak appeared at 1615 cm^{-1}, attributed to the C=C skeletal vibration mode of the graphitic domains, and two small peaks at ~1220 and 1430 cm^{-1}, assigned to the C-O-C and C-OH vibration modes, respectively, signifying the presence of a few remaining oxygen containing functionalities after the reduction of GO. In the XRD patterns of the samples, the characteristic diffraction peaks of the TiO_2 anatase phase were detected before and after modification with the graphitic sheets (Figure S5). However, the diffraction peaks of rGO were not evident after the surface modification of TiO_2, because rGO exhibits a main peak at 24.5°, which overlaps with the TiO_2 peak at 25.4°. More importantly, the surface modification of TiO_2 with the graphitic sheets induced a red shift in the absorption edge of TiO_2, resulting in a band gap energy narrowing from 3.2 eV, for the bare TiO_2 nanoparticles, to 3 eV for the rGO-modified TiO_2 nanoparticles (Figure S5), which extends the absorption of the composite material in the visible range of the spectrum.

The hybrid material was prepared by the addition of an appropriate amount of the rGO-modified TiO_2 nanoparticle dispersion, in a 1:1 EtOH:H_2O mixture, to a solution of modified chitosan in the same solvent. The mixture was stirred and sonicated for at least 10 min to ensure the complete dispersion of the rGO-modified TiO_2 nanoparticles. Next, a solution of the cross-linker in methanol, was added. The composition of the material was 2wt% rGO-modified TiO_2 nanoparticles with respect to the modified chitosan and 5mol% cross-linker with respect to the monomer repeats units of the biopolymer. Following dilution with a 1:1 EtOH:H_2O mixture to

obtain a 1 mg mL^{-1} concentration, the solution of the hybrid material was drop-casted onto glass substrates modified with GOPTES, which enables the covalent binding of the polymer onto the substrate. After solvent evaporation, the samples were baked at 110 ^{o}C overnight, to promote the reaction of the alkyl bromide functionalities of the cross-linker with the free amino groups of chitosan and form the polymer network. Simultaneously, the amine groups of chitosan reacted with the glycidyl groups of the substrate to covalently bind the hybrid coating on the substrate. After washing with ethanol, films of 400-700 nm thickness, as determined by ellipsometry, were obtained. The water contact angles on the hybrid films were measured at ~40^{o} signifying a moderately hydrophilic surface.

The UV/vis spectra of the hybrid films exhibited an increase in the absorbance below 450 nm, suggesting the successful incorporation of the rGO-modified TiO_2 nanoparticles within the modified chitosan matrix (Figure 2).

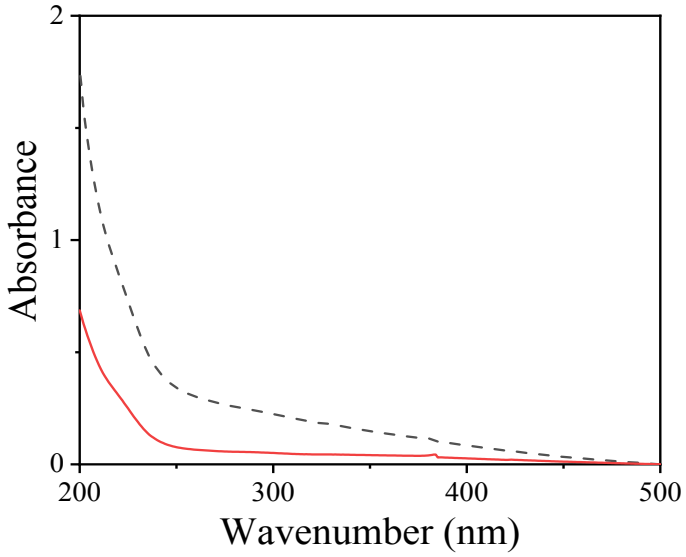

Figure 2: UV-Vis spectra of the cross-linked modified chitosan film (red solid line) and the cross-linked hybrid thin film (black dashed line).

Antimicrobial activity of the hybrid films

The antimicrobial activity of the hybrid thin films in the dark and under visible light irradiation was evaluated using the PCM. Two representative Gram-positive and Gram-negative bacteria, *B. cereus* and *E. coli*, respectively were tested. A bacterial suspension of 10^8 CFU/ml was used for both bacteria strains and was inoculated on the sample surfaces at 37 °C for 5 h. A bare glass substrate was used as the control surface.

Figure 3 shows the logarithmic reduction in bacteria growth for both bacterial strains (*B. cereus* and *E. coli*) after 5 h contact with the hybrid coatings in the dark and under visible light irradiation. For *B. cereus*, the hybrid coatings exhibited a ~3log reduction of the viable bacteria in the dark, signifying a strong biocidal action, whereas for *E. coli*, the bacterial reduction was slightly lower at ~1.8log. The lower antimicrobial activity against the Gram-negative microorganisms is attributed to its much-complicated cell membrane comprising an extra peptidoglycan layer, which seals a higher protection to the integrity of the bacteria structure.[49-50] On the other hand, under visible light irradiation, the antibacterial activity of the hybrid coatings was significantly enhanced to 6log and 5log reduction in the growth of *B. cereus* and *E. coli*, respectively (Figure3), verifying the strong biocidal activity of the rGO-modified TiO_2 nanoparticles in the hybrid film. The pronounced antimicrobial activity of the hybrid coatings under visible light irradiation is attributed to the combined action of the positively charged QAS moieties of chitosan, which interact with the negatively charged bacterial cell membranes, causing their destabilization, and the reactive oxygen species (ROS) produced by the rGO-modified TiO_2 nanoparticles, which cause the oxidative damage of the cell membrane, cell distortion and lysis and eventually cell death. This “synergistic” antibacterial effect promotes a very strong contact-killing activity of the films against bacterial infections.

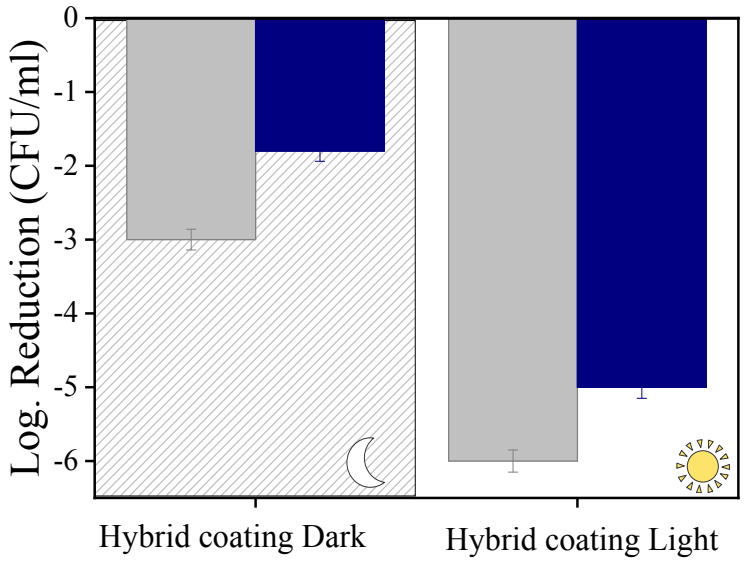

Figure 3. Bactericidal activity of the hybrid coatings after 5 h contact with *B. cereus* (gray bars) and *E. coli* (blue bars) at 37 °C in the dark and under visible light irradiation. Each bar represents the log reduction from 3 different experiments carried out in duplicates (mean ± SD).

SEM was used to monitor the morphological changes of the bacteria after 5 h contact with the hybrid coatings and thus to elucidate the mechanism of antimicrobial action. Figure 4 shows typical SEM images of *E. coli* and *B. cereus* attached on a glass substrate following visible light irradiation and on the hybrid coatings in the dark and after visible light irradiation. Intact bacteria with a clear rod-like shape were observed for both *E. coli* and *B. cereus* on the bare glass surface after visible light irradiation (Figures 4a and 4d). In contrast, the bacteria attached on the hybrid coatings in the dark (Figures 4b and 4e) suffered severe damage of their cellular envelope, and lost the integrity of their membrane. This indicates that the cationic QAS moieties present along the chitosan backbone interact strongly with the microbe cell membranes and kill the bacteria by the lysis of their cytoplasm, in agreement with the PCM results discussed above. After irradiation with visible light, the synergistic antimicrobial action of the rGO-modified TiO_2 nanoparticles and the cationic QAS moieties of chitosan resulted in

the complete damage of the cell membrane and the lysis of the bacterial cells (Figures 4c and 4f). The major reason for the visible light damage of the bacterial cells, exposed to the photocatalytic rGO-modified TiO_2 nanoparticles, is the disruption of their outer membrane by the produced ROS which impairs the bacteria at relatively low exposures.[51-52]

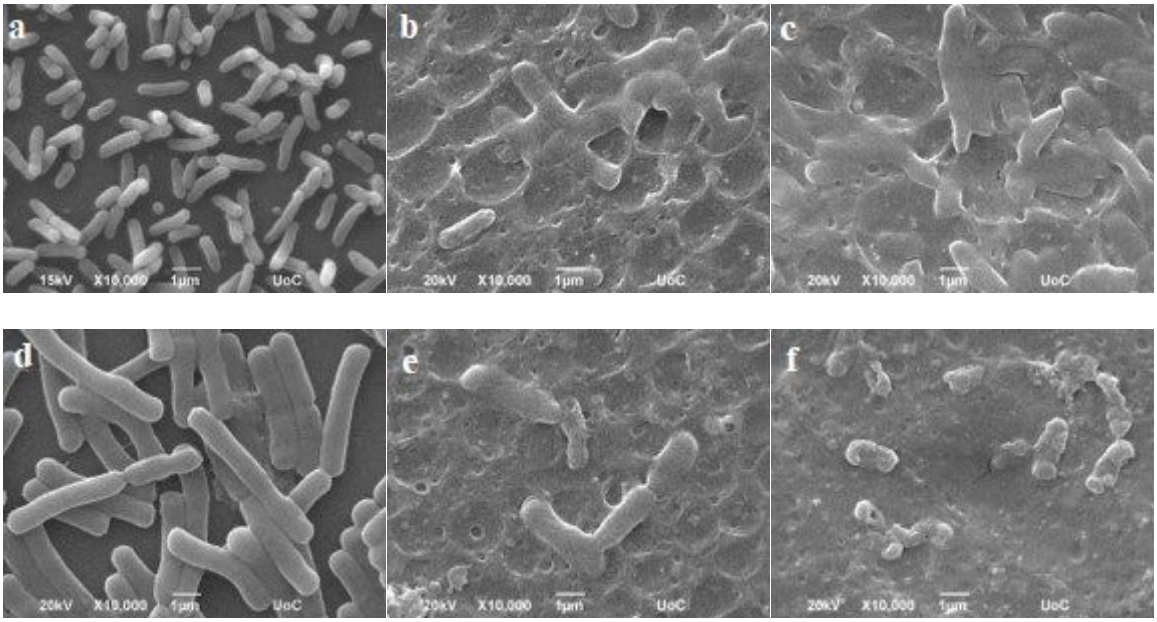

Figure 4. SEM images of *E. coli* (a, b, c) and *B. cereus* (e, f, g) attached on bare glass substrates after 5 h contact under visible light irradiation (a, d) and on the hybrid coatingsafter5 h contact in the dark (b, e) and under visible light irradiation (c, f).

The viability of the attached bacterial cells on the hybrid coatings was determined by a LIVE/DEAD assay. SYTO 9, which exhibits a characteristic green fluorescence upon staining the intact cell membranes, and propidium iodide, which stains red the non-viable bacteria cells, were used in this assay. Figure 5 shows characteristic CLSM images of the bacteria on glass substrates and on the hybrid films after visible light irradiation. The bacteria attached on the glass substrates are alive (Figures 5a and 5c), exhibiting the characteristic green color, whereas, the bacteria on the hybrid coatings appear mostly red (Figures 5b and 5d) signifying a significantly reduced viability for both bacteria stains, in good agreement with the PCM and SEM findings discussed above.

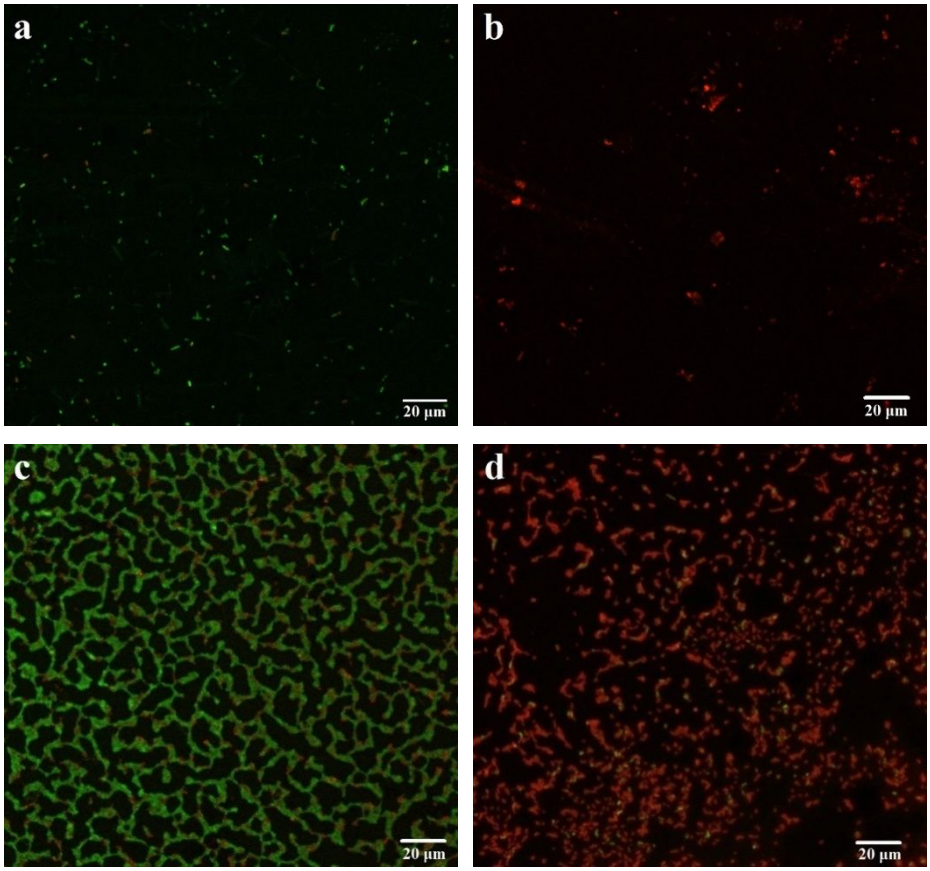

Figure 5. CLSM images of *E. coli* (a, b) and *B. cereus* (c, d) attached on glass (a, c) and on the hybrid films (b, d), after 5 h contact with the surfaces under visible light irradiation. The green and red colors denote alive and dead bacteria, respectively**.**

From the above results, one can conclude that the hybrid coatings exhibit an excellent bactericidal performance under visible light irradiation, due to the "synergistic" action of the cationic QAS moieties of the polymer and the rGO-modified TiO_2 nanoparticles, and can qualify as profoundly infection-resistant surfaces, which are attractive for use in numerous applications.

Self-renewable behavior of the hybrid film surface

The self-polishing properties of the hybrid films were studied by following the changes in the film thickness, by FTIR spectroscopy, as a function of immersion time in water of different pH

values ranging from pH 2 to 8 (Figure6). A decrease in the film thickness with the immersion time was found which was dependent on the solution pH. At pH 2 and 3, the films were completely removed from the substrate after 3 days immersion in the medium, whereas at pH 4 and 5 the dissolution of the film was prolonged to 7 days. More importantly, a significant decrease in the film polishing rate was found at pH 6, with the hybrid coating retaining 30 % of its initial thickness after 60 days immersion time. Finally, the film dissolution rate was reduced further at pH 7 and 8, at which a decrease in thickness of only 24 % and 16 %, respectively, was measured after 60 days immersion time. This self-polishing behavior of the hybrid films is attributed to the acid hydrolysis of the acetal-based cross-linker, which leads to the dissolution of the polymer and its removal from the film. The rate of acid hydrolysis of the acetal bonds, to produce acetaldehyde and hydroxy products, depends on the pH of the solution, leading to the observed differences in the decrease of the film thickness as a function of immersion time for the different media.

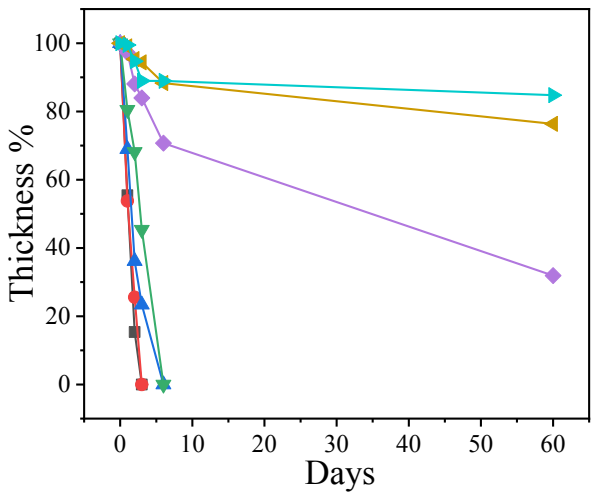

Figure 6. % thickness of the hybrid films as a function of immersion time in water at different pH values.pH 2 – black squares, pH 3 – red circles, pH 4 –blue triangles up, pH 5 – greentriangles down, pH 6 –purple rhombi, pH 7 –yellow triangles left and pH 8 –light blue triangles right.

The self-polishing behavior of the hybrid films enables the progressive removal of the top layer of the film, which eliminates the deposited dead bacteria and the debris from the surface of the coating, leading to the renewal of its antimicrobial action in a "kill-and-release" approach using pH as an external stimulus (Figure 7). In addition, the peeling of the film at media around neutral pH values enables the application of the coatings under physiological and biologically-relevant conditions, not requiring extreme acidic or basic media. The proposed approach comprises a promising strategy, for the development of biocompatible surfaces, which prevent initial bacterial attachment and subsequent biofilm formation, exhibiting a long-term antibacterial activity. [53-54]

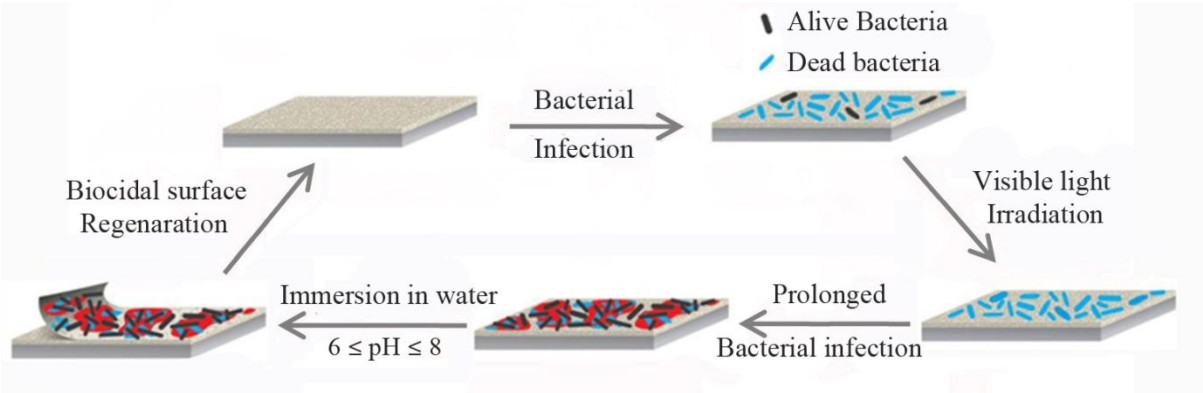

Figure 7: Schematic representation of the biocidal action and the self-polishing behavior of the hybrid coatings allowing the renewal of their antimicrobial activity.

Conclusions

Novel hybrid coatings combining enhanced biocidal properties with long-term, self-renewable antimicrobial action were prepared. The films were based on a natural polymer, chitosan, modified to bear QAS groups that function as permanent biocidal moieties, and rGO-modified TiO_2 nanoparticles, which exhibit effective antimicrobial action under visible light irradiation. Cross-linking of the polymer was induced by an acetal-based, acid-degradable cross-linker

which reacted with the amine groups of chitosan. The hybrid coatings were evaluated for their biocidal properties under dark and visible light irradiation using Gram-positive and Gram-negative bacteria strains. The films exhibited an effective biocidal efficacy in the dark against Gram-negative (98 % killing of *E. coli*) and Gram-positive (99.9 % killing of *B. cereus*) microorganisms, attributed to the QAS moieties of chitosan, and an excellent antimicrobial performance under visible light irradiation (99,999 % killing of *E. coli* and 99,9999 % killing of *B. Cereus*) due to the synergistic action of the ROS produced by the rGO-modified TiO_2 nanoparticles, and the QAS groups of the polymer.

The hybrid films exhibited a self-polishing behavior upon immersion in water, which was determined by the solution pH. In highly acidic media (pH 2 to 5), the films were completely removed from the substrates in less than one week, whereas in mild acidic (pH 6), neutral (pH 7) and slightly basic (pH 8) water, a gradual decrease in film thickness was found, with only the top 70 %, 24 % and 16 % of the polymer layer, respectively, being removed after 60 days immersion time. This was attributed to the pH-dependent hydrolysis rate of the acetal-based cross-linker, and led to a pH-responsive renewal of the film surface, which prolongs the antibacterial activity of the coatings.

Acknowledgements

This research has been financed by the Operational Program "Human Resources Development, Education and Lifelong Learning" and is co-financed by the European Union (European Social Fund) and Greek national funds (program MIS 5006044). The authors acknowledge Ms Aleka Manousaki for technical assistance with the SEM characterization.

References

(1) Campoccia, D.; Speziale, P.; Ravaioli, S.; Cangini, I.; Rindi, S.; Pirini, V.; Montanaro, L.; Arciola, C. R. The presence of both bone sialoprotein-binding protein gene and collagen adhesin gene as a typical virulence trait of the major epidemic cluster in isolates from orthopedic implant infections. *Biomaterials* **2009,** *30* (34), 6621-8, DOI: 10.1016/j.biomaterials.2009.08.032.

(2) Hoiby, N.; Bjarnsholt, T.; Givskov, M.; Molin, S.; Ciofu, O. Antibiotic resistance of bacterial biofilms. *Int. J. Antimicrob. Agents* **2010,** *35* (4), 322-32, DOI: 10.1016/j.ijantimicag.2009.12.011.

(3) Shaikh, S.; Fatima, J.; Shakil, S.; Rizvi, S. M.; Kamal, M. A. Antibiotic resistance and extended spectrum beta-lactamases: Types, epidemiology and treatment. *Saudi J. Biol. Sci.* **2015,** *22* (1), 90-101, DOI: 10.1016/j.sjbs.2014.08.002.

(4) Speziale, P.; Pietrocola, G.; Rindi, S.; Provenzano, M.; Provenza, G.; Di Poto, A.; Visai, L.; Arciola, C. R. Structural and functional role of Staphylococcus aureus surface components recognizing adhesive matrix molecules of the host. *Future Microbiol.* **2009,** *4* (10), 1337-52, DOI: 10.2217/fmb.09.102.

(5) Banerjee, I.; Pangule, R. C.; Kane, R. S. Antifouling coatings: recent developments in the design of surfaces that prevent fouling by proteins, bacteria, and marine organisms. *Adv. Mater.* **2011,** *23* (6), 690-718, DOI: 10.1002/adma.201001215.

(6) Liu, S.; Zheng, J.; Hao, L.; Yegin, Y.; Bae, M.; Ulugun, B.; Taylor, T. M.; Scholar, E. A.; Cisneros-Zevallos, L.; Oh, J. K.; Akbulut, M. Dual-Functional, Superhydrophobic Coatings with Bacterial Anticontact and Antimicrobial Characteristics. *ACS Appl. Mater. Interfaces* **2020**, DOI: 10.1021/acsami.9b18928.

(7) Kugel, A.; Stafslien, S.; Chisholm, B. J. Antimicrobial coatings produced by "tethering" biocides to the coating matrix: A comprehensive review. *Prog. Org. Coat.* **2011,** *72* (3), 222-252, DOI: 10.1016/j.porgcoat.2011.07.004.

(8) Hasan, J.; Crawford, R. J.; Ivanova, E. P. Antibacterial surfaces: the quest for a new generation of biomaterials. *Trends Biotechnol.* **2013,** *31* (5), 295-304, DOI: https://doi.org/10.1016/j.tibtech.2013.01.017.

(9) Akhavan, O.; Ghaderi, E. Cu and CuO nanoparticles immobilized by silica thin films as antibacterial materials and photocatalysts. *Surf. Coat. Technol.* **2010,** *205* (1), 219-223, DOI: 10.1016/j.surfcoat.2010.06.036.

(10) Bai, X. Y.; Li, L. L.; Liu, H. Y.; Tan, L. F.; Liu, T. L.; Meng, X. W. Solvothermal Synthesis of ZnO Nanoparticles and Anti-Infection Application in Vivo. *ACS Appl. Mater. Interfaces* **2015,** *7* (2), 1308-1317, DOI: 10.1021/am507532p.

(11) Benetti, G.; Cavaliere, E.; Brescia, R.; Salassi, S.; Ferrando, R.; Vantomme, A.; Pallecchi, L.; Pollini, S.; Boncompagni, S.; Fortuni, B.; Van Bael, M. J.; Banfi, F.; Gavioli, L. Tailored Ag-Cu-Mg multielemental nanoparticles for wide-spectrum antibacterial coating. *Nanoscale* **2019,** *11* (4), 1626-1635, DOI: 10.1039/c8nr08375d.

(12) Kumar, R.; Anandan, S.; Hembram, K.; Rao, T. N. Efficient ZnO-Based Visible-Light-Driven Photocatalyst for Antibacterial Applications. *ACS Appl. Mater. Interfaces* **2014,** *6* (15), 13138-13148, DOI: 10.1021/am502915v.

(13) Rtimi, S.; Dionysiou, D. D.; Pillai, S. C.; Kiwi, J. Advances in catalytic/photocatalytic bacterial inactivation by nano Ag and Cu coated surfaces and medical devices. *Appl. Catal. B* **2019,** *240*, 291-318, DOI: 10.1016/j.apcatb.2018.07.025.

(14) Bonomo, R. A. Multiple antibiotic-resistant bacteria in long-term-care facilities: An emerging problem in the practice of infectious diseases. *Clinical infectious diseases : an*

official publication of the Infectious Diseases Society of America **2000,** *31* (6), 1414-22, DOI: 10.1086/317489.

(15) Josset, S.; Keller, N.; Lett, M. C.; Ledoux, M. J.; Keller, V. Numeration methods for targeting photoactive materials in the UV-A photocatalytic removal of microorganisms. *Chem. Soc. Rev.* **2008,** *37* (4), 744-55, DOI: 10.1039/b711748p.

(16) Banerjee, S.; Dionysiou, D. D.; Pillai, S. C. Self-cleaning applications of TiO2 by photo-induced hydrophilicity and photocatalysis. *Appl. Catal. B* **2015,** *176*, 396-428, DOI: 10.1016/j.apcatb.2015.03.058.

(17) Kubacka, A.; Diez, M. S.; Rojo, D.; Bargiela, R.; Ciordia, S.; Zapico, I.; Albar, J. P.; Barbas, C.; dos Santos, V. A. P. M.; Fernandez-Garcia, M.; Ferrer, M. Understanding the antimicrobial mechanism of TiO2-based nanocomposite films in a pathogenic bacterium. *Sci. Rep.* **2014,** *4*, DOI: 10.1038/Srep04134.

(18) Koufakis, E.; Manouras, T.; Anastasiadis, S. H.; Vamvakaki, M. Film Properties and Antimicrobial Efficacy of Quaternized PDMAEMA Brushes: Short vs Long Alkyl Chain Length. *Langmuir* **2020,** *36* (13), 3482-3493, DOI: 10.1021/acs.langmuir.9b03266.

(19) Parkatzidis, K.; Chatzinikolaidou, M.; Koufakis, E.; Kaliva, M.; Farsari, M.; Vamvakaki, M. Multi-photon polymerization of bio-inspired, thymol-functionalized hybrid materials with biocompatible and antimicrobial activity. *Polym. Chem.* **2020**, DOI: 10.1039/D0PY00281J.

(20) Zhang, L. J.; Gallo, R. L. Antimicrobial peptides. *Curr. Biol.* **2016,** *26* (1), R14-R19, DOI: DOI 10.1016/j.cub.2015.11.017.

(21) Kenawy, E.-R.; Kandil, S. CHAPTER 3 Synthesis, Antimicrobial Activity and Applications of Polymers with Ammonium and Phosphonium Groups. In *Polymeric Materials with Antimicrobial Activity: From Synthesis to Applications*; The Royal Society of Chemistry: 2014; pp 54-74.

(22) Xue, Y.; Xiao, H. N.; Zhang, Y. Antimicrobial Polymeric Materials with Quaternary Ammonium and Phosphonium Salts. *Int. J. Mol. Sci.* **2015,** *16* (2), 3626-3655, DOI: 10.3390/ijms16023626.

(23) Maia, J.; Carvalho, R. A.; Coelho, J. F. J.; Simoes, P. N.; Gil, M. H. Insight on the periodate oxidation of dextran and its structural vicissitudes. *Polymer* **2011,** *52* (2), 258-265, DOI: 10.1016/j.polymer.2010.11.058.

(24) Ulery, B. D.; Nair, L. S.; Laurencin, C. T. Biomedical Applications of Biodegradable Polymers. *J. Polym. Sci. B Polym. Phys.* **2011,** *49* (12), 832-864, DOI: 10.1002/polb.22259.

(25) Sahariah, P.; Masson, M. Antimicrobial Chitosan and Chitosan Derivatives: A Review of the Structure-Activity Relationship. *Biomacromolecules* **2017,** *18* (11), 3846-3868, DOI: 10.1021/acs.biomac.7b01058.

(26) Muzzarelli, R.; Tarsi, R.; Filippini, O.; Giovanetti, E.; Biagini, G.; Varaldo, P. E. Antimicrobial Properties of N-Carboxybutyl Chitosan. *Antimicrob. Agents Chemother.* **1990,** *34* (10), 2019-2023, DOI: Doi 10.1128/Aac.34.10.2019.

(27) Helander, I. M.; Nurmiaho-Lassila, E. L.; Ahvenainen, R.; Rhoades, J.; Roller, S. Chitosan disrupts the barrier properties of the outer membrane of Gram-negative bacteria. *Int. J. Food Microbiol.* **2001,** *71* (2-3), 235-244, DOI: Doi 10.1016/S0168-1605(01)00609-2.

(28) Lim, S. H.; Hudson, S. M. Review of chitosan and its derivatives as antimicrobial agents and their uses as textile chemicals. *J. Macromol.Sci.-Pol. Rev.* **2003,** *C43* (2), 223-269, DOI: 10.1081/Mc-120020161.

(29) Prashanth, K. V. H.; Tharanathan, R. N. Chitin/chitosan: modifications and their unlimited application potential - an overview. *Trends Food Sci. Tech.* **2007,** *18* (3), 117-131, DOI: 10.1016/j.tifs.2006.10.022.

(30) Konwar, A.; Kalita, S.; Kotoky, J.; Chowdhury, D. Chitosan-Iron Oxide Coated Graphene Oxide Nanocomposite Hydrogel: A Robust and Soft Antimicrobial Biofilm. *ACS Appl. Mater. Interfaces* **2016,** *8* (32), 20625-20634, DOI: 10.1021/acsami.6b07510.

(31) Petkova, P.; Francesko, A.; Fernandes, M. M.; Mendoza, E.; Perelshtein, I.; Gedanken, A.; Tzanov, T. Sonochemical Coating of Textiles with Hybrid ZnO/Chitosan Antimicrobial Nanoparticles. *ACS Appl. Mater. Interfaces* **2014,** *6* (2), 1164-1172, DOI: 10.1021/am404852d.

(32) Tripathy, A.; Pahal, S.; Mudakavi, R. J.; Raichur, A. M.; Varma, M. M.; Sen, P. Impact of Bioinspired Nanotopography on the Antibacterial and Antibiofilm Efficacy of Chitosan. *Biomacromolecules* **2018,** *19* (4), 1340-1346, DOI: 10.1021/acs.biomac.8b00200.

(33) Hosseinnejad, M.; Jafari, S. M. Evaluation of different factors affecting antimicrobial properties of chitosan. *Int. J. Biol. Macromol.* **2016,** *85*, 467-475, DOI: https://doi.org/10.1016/j.ijbiomac.2016.01.022.

(34) Khattak, S.; Wahid, F.; Liu, L.-P.; Jia, S.-R.; Chu, L.-Q.; Xie, Y.-Y.; Li, Z.-X.; Zhong, C. Applications of cellulose and chitin/chitosan derivatives and composites as antibacterial materials: current state and perspectives. *Appl. Microbiol. Biotechnol.* **2019,** *103* (5), 1989-2006, DOI: 10.1007/s00253-018-09602-0.

(35) Wei, T.; Tang, Z. C.; Yu, Q.; Chen, H. Smart Antibacterial Surfaces with Switchable Bacteria-Killing and Bacteria-Releasing Capabilities. *ACS Appl. Mater. Interfaces* **2017,** *9* (43), 37511-37523, DOI: 10.1021/acsami.7b13565.

(36) Yu, Q.; Wu, Z. Q.; Chen, H. Dual-function antibacterial surfaces for biomedical applications. *Acta Biomater.* **2015,** *16*, 1-13, DOI: 10.1016/j.actbio.2015.01.018.

(37) Cao, Z. Q.; Mi, L.; Mendiola, J.; Ella-Menye, J. R.; Zhang, L.; Xue, H.; Jiang, S. Y. Reversibly Switching the Function of a Surface between Attacking and Defending against Bacteria. *Angew .Chem. Int. Ed.* **2012,** *51* (11), 2602-2605, DOI: 10.1002/anie.201106466.

(38) Shi, Z. Q.; Cai, Y. T.; Deng, J.; Zhao, W. F.; Zhao, C. S. Host-Guest Self-Assembly Toward Reversible Thermoresponsive Switching for Bacteria Killing and Detachment. *ACS Appl. Mater. Interfaces* **2016,** *8* (36), 23523-23532, DOI: 10.1021/acsami.6b07397.

(39) Wei, T.; Zhan, W. J.; Yu, Q.; Chen, H. Smart Biointerface with Photoswitched Functions between Bactericidal Activity and Bacteria-Releasing Ability. *ACS Appl. Mater. Interfaces* **2017,** *9* (31), 25767-25774, DOI: 10.1021/acsami.7b06483.

(40) Yu, Q.; Cho, J.; Shivapooja, P.; Ista, L. K.; Lopez, G. P. Nanopatterned Smart Polymer Surfaces for Controlled Attachment, Killing, and Release of Bacteria. *ACS Appl. Mater. Interfaces* **2013,** *5* (19), 9295-9304, DOI: 10.1021/am4022279.

(41) Yu, Q.; Ge, W. Y.; Atewologun, A.; Lopez, G. P.; Stiff-Roberts, A. D. RIR-MAPLE deposition of multifunctional films combining biocidal and fouling release properties. *J. Mater. Chem. B* **2014,** *2* (27), 4371-4378, DOI: 10.1039/c4tb00566j.

(42) Yu, Q.; Ge, W. Y.; Atewologun, A.; Stiff-Roberts, A. D.; Lopez, G. P. Antimicrobial and bacteria-releasing multifunctional surfaces: Oligo (p-phenylene-ethynylene)/poly (N-isopropylacrylamide) films deposited by RIR-MAPLE. *Colloids Surf. B. Biointerfaces* **2015,** *126*, 328-334, DOI: 10.1016/j.colsurfb.2014.12.043.

(43) Wang, Y.; Wei, T.; Qu, Y.; Zhou, Y.; Zheng, Y.; Huang, C.; Zhang, Y.; Yu, Q.; Chen, H. Smart, Photothermally Activated, Antibacterial Surfaces with Thermally Triggered Bacteria-Releasing Properties. *ACS Appl. Mater. Interfaces* **2019**, DOI: 10.1021/acsami.9b17581.

(44) Yan, S. J.; Shi, H. C.; Song, L. J.; Wang, X. H.; Liu, L.; Luan, S. F.; Yang, Y. M.; Yin, J. H. Nonleaching Bacteria-Responsive Antibacterial Surface Based on a Unique Hierarchical. *ACS Appl. Mater. Interfaces* **2016,** *8* (37), 24471-24481, DOI: 10.1021/acsami.6b08436.

(45) Wang, C. C.; Ying, J. Y. Sol-gel synthesis and hydrothermal processing of anatase and rutile titania nanocrystals. *Chem. Mater.* **1999,** *11* (11), 3113-3120, DOI: Doi 10.1021/Cm990180f.

(46) Poh, H. L.; Sanek, F.; Ambrosi, A.; Zhao, G. J.; Sofer, Z.; Pumera, M. Graphenes prepared by Staudenmaier, Hofmann and Hummers methods with consequent thermal exfoliation exhibit very different electrochemical properties. *Nanoscale* **2012,** *4* (11), 3515-3522, DOI: 10.1039/c2nr30490b.

(47) Zhang, H.; Lv, X. J.; Li, Y. M.; Wang, Y.; Li, J. H. P25-Graphene Composite as a High Performance Photocatalyst. *Acs Nano* **2010,** *4* (1), 380-386, DOI: 10.1021/nn901221k.

(48) Kim, S. Competitive Biological Activities of Chitosan and Its Derivatives: Antimicrobial, Antioxidant, Anticancer, and Anti-Inflammatory Activities. *Int. J. Polym. Sci.* **2018**, DOI: 10.1155/2018/1708172.

(49) Pant, J.; Gao, J.; Goudie, M. J.; Hopkins, S. P.; Locklin, J.; Handa, H. A multi-defense strategy: Enhancing bactericidal activity of a medical grade polymer with a nitric oxide donor and surface-immobilized quaternary ammonium compound. *Acta Biomater.* **2017,** *58*, 421-431, DOI: https://doi.org/10.1016/j.actbio.2017.05.061.

(50) Roy, H. Tuning the properties of the bacterial membrane with aminoacylated phosphatidylglycerol. *IUBMB Life* **2009,** *61* (10), 940-953, DOI: 10.1002/iub.240.

(51) Nagay, B. E.; Dini, C.; Cordeiro, J. M.; Ricomini-Filho, A. P.; de Avila, E. D.; Rangel, E. C.; da Cruz, N. C.; Barao, V. A. R. Visible-Light-Induced Photocatalytic and Antibacterial Activity of TiO2 Codoped with Nitrogen and Bismuth: New Perspectives to Control Implant-Biofilm-Related Diseases. *ACS Appl. Mater. Interfaces* **2019,** *11* (20), 18186-18202, DOI: 10.1021/acsami.9b03311.

(52) Nica, I. C.; Stan, M. S.; Popa, M.; Chifiriuc, M. C.; Pircalabioru, G. G.; Lazar, V.; Dumitrescu, I.; Diamandescu, L.; Feder, M.; Baibarac, M.; Cernea, M.; Maraloiu, V. A.; Popescu, T.; Dinischiotu, A. Development and Biocompatibility Evaluation of Photocatalytic TiO(2)/Reduced Graphene Oxide-Based Nanoparticles Designed for Self-Cleaning Purposes. *Nanomaterials* **2017,** *7* (9), DOI: 10.3390/nano7090279.

(53) Lu, Y. M.; Wu, Y.; Liang, J.; Libera, M. R.; Sukhishvili, S. A. Self-defensive antibacterial layer-by-layer hydrogel coatings with pH-triggered hydrophobicity. *Biomaterials* **2015,** *45*, 64-71, DOI: 10.1016/j.biomaterials.2014.12.048.

(54) Wang, F. L.; Raval, Y.; Chen, H. Y.; Tzeng, T. R. J.; DesJardins, J. D.; Anker, J. N. Development of Luminescent pH Sensor Films for Monitoring Bacterial Growth Through Tissue. *Adv. Healthcare Mater.* **2014,** *3* (2), 197-204, DOI: 10.1002/adhm.201300101.

FOR TOC USE ONLY

TOC Image